EUKARYOTIC CELL, May 2009, p. 723–731 Vol. 8, No. 5
1535-9778/09/$08.00+0 doi:10.1128/EC.00018-09

Microtubule-Nucleus Interactions in *Dictyostelium discoideum* Mediated by Central Motor Kinesins▽†

Irina Tikhonenko,[1] Dilip K. Nag,[1,2] Douglas N. Robinson,[3] and Michael P. Koonce[1,2]*

Division of Translational Medicine, Wadsworth Center, Albany, New York 12201-0509[1]; Department of Biomedical Sciences, School of Public Health, University at Albany, Albany, New York 12201-0509[2]; and Department of Cell Biology, Johns Hopkins University School of Medicine, Baltimore, Maryland 21205[3]

Received 12 January 2009/Accepted 10 March 2009

Kinesins are a diverse superfamily of motor proteins that drive organelles and other microtubule-based movements in eukaryotic cells. These motors play important roles in multiple events during both interphase and cell division. *Dictyostelium discoideum* contains 13 kinesin motors, 12 of which are grouped into nine families, plus one orphan. Functions for 11 of the 13 motors have been previously investigated; we address here the activities of the two remaining kinesins, both isoforms with central motor domains. Kif6 (of the kinesin-13 family) appears to be essential for cell viability. The partial knockdown of Kif6 with RNA interference generates mitotic defects (lagging chromosomes and aberrant spindle assemblies) that are consistent with kinesin-13 disruptions in other organisms. However, the orphan motor Kif9 participates in a completely novel kinesin activity, one that maintains a connection between the microtubule-organizing center (MTOC) and nucleus during interphase. *kif9* null cell growth is impaired, and the MTOC appears to disconnect from its normally tight nuclear linkage. Mitotic spindles elongate in a normal fashion in *kif9*$^-$ cells, but we hypothesize that this kinesin is important for positioning the MTOC into the nuclear envelope during prophase. This function would be significant for the early steps of cell division and also may play a role in regulating centrosome replication.

Directed cell migration, organelle transport, and cell division involve fundamental motilities that are necessary for eukaryotic cell viability and function. Much of the force required for these motilities is generated through the cyclical interactions of motor proteins with the cell cytoskeleton. Microtubules (MTs) and actin filaments provide structural support and directional guides, and all eukaryotic organisms have diverse, often extensive families of motors that carry out different tasks. Functional studies have revealed that many of the motors work in combination with others, and that the individual deletion of a single motor activity often is insufficient to produce a defect that substantially impairs cell growth or function. The latter phenomenon is particularly evident in some organisms with simple motor families (14, 42). By contrasting homologous motor functions between simple and complex systems, we hope to learn the details of how each motor is custom-tuned for specific tasks.

Dictyostelium discoideum is a compact amoeba that exhibits robust forms of motility common to nearly all animal cells, with speeds that frequently exceed corresponding rates in vertebrate cell models (25, 33, 54). Since *Dictyostelium* possesses a relatively small number of motor proteins (13 kinesin, 1 dynein, and 13 myosin isoforms [23, 24, 26]), it combines advantages of terrific cytology with straightforward molecular genetics and thus represents an excellent model to investigate individual and combined motor protein actions. To date, 11 of the 13 kinesin motors have been analyzed functionally (5, 17, 18, 30, 42, 46, 51, 60). Only 1 of these 11 motors, Kif3, a member of the kinesin-1 family of organelle transporters, appears to be essential for organism viability (51). Individual disruptions of three kinesin genes (*kif1*, *kif4*, and *kif12*) produce distinctive defects in cell growth or organelle transport (30, 42, 46). Analyses of six of the seven other kinesins reveal important phenotypes but only when combined with other motor disruptions or cell stresses. We address here the roles of the remaining two *Dictyostelium* MT-based motors.

kif6 and *kif9* encode two central motor kinesins in the *Dictyostelium* genome (24). The best-studied isoforms of this motor type are represented by the kinesin-13 family, and they largely function to regulate MT length during cell division (13, 16, 40, 41). In some organisms, kinesin-13 motors also have been shown to operate during interphase and to mediate MT and flagellar length control (3, 4, 15) and perhaps even organelle transport (32, 43, 56). *kif6* encodes the kinesin-13 family member in *Dictyostelium*. We demonstrate that Kif6 activity is essential for viability, and that it plays a primary, conserved role in chromosome segregation during cell division.

The second of the central motor kinesins, Kif9, does not group with an existing family (24, 38). The gene disruption of this motor reveals a completely novel function for a kinesin in maintaining a connection between the MT-organizing center (MTOC) and the nucleus. By electron microscopy (EM), the MTOC of *Dictyostelium* appears as a cytoplasmic cube-shaped structure surrounded by amorphous dense material (39, 44). EM, biochemical analyses, antibody labeling, and live-cell imaging studies have demonstrated that during interphase, the cytoplasmic MTOC is firmly and closely attached to the nucleus (28, 29, 44, 48, 49, 63). Upon entry into mitosis, the

* Corresponding author. Mailing address: Wadsworth Center, Empire State Plaza, P.O. Box 509, Albany, NY 12201-0509. Phone: (518) 486-1490. Fax: (518) 474-7992. E-mail: Koonce@wadsworth.org.

† Supplemental material for this article may be found at http://ec.asm.org/.

▽ Published ahead of print on 13 March 2009.

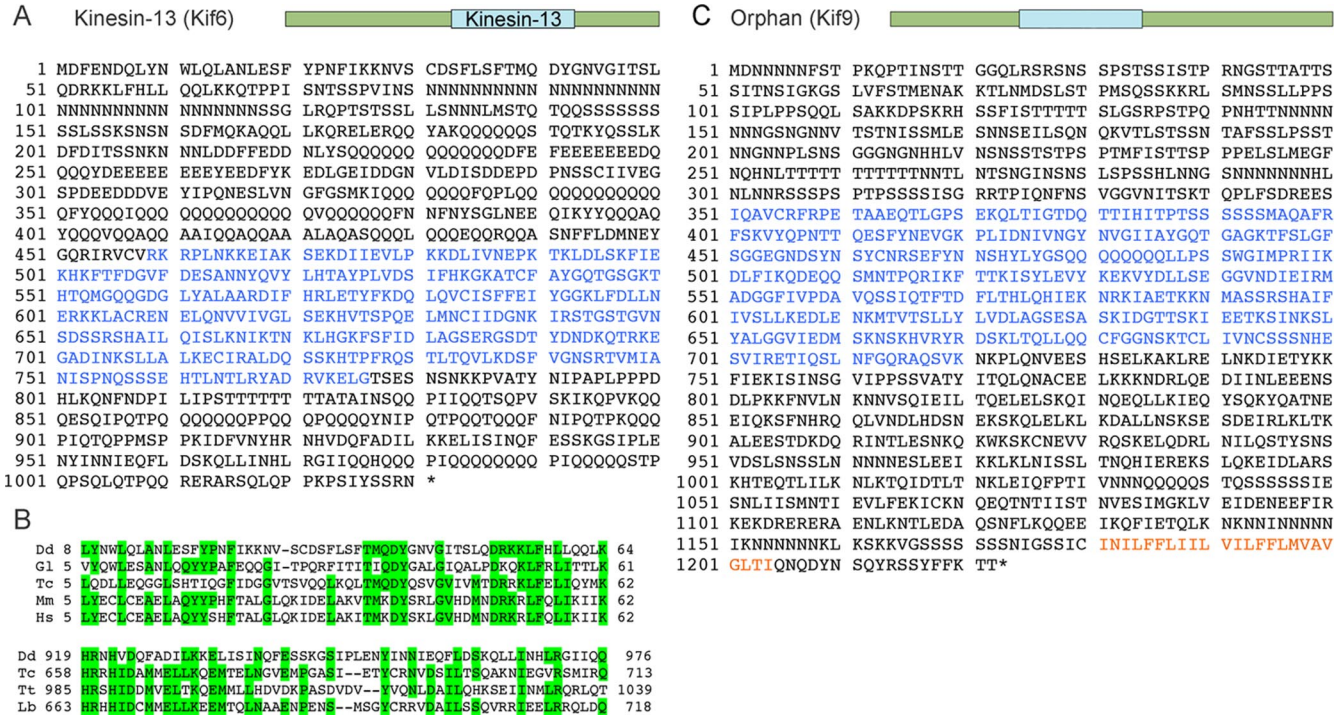

FIG. 1. Sequence analysis of the two central motor kinesins of *Dictyostelium*. (A) Cartoon graphic and sequence of Kif6 (kinesin-13). The motor domain is highlighted in blue. Note the extensive repetition of amide residues (N and Q). (B) Conserved domain alignments at the amino-terminal and carboxy-terminal regions of the Kif6 polypeptide. Green boxes highlight identical residues in at least three sequences. Dd, *Dictyostelium discoideum* (DDB0191499); Gl, *Giardia lamblia* (XP_001709959.1); Tc, *Trypanosoma cruzi* (XP_808344.1); Mm, *Mus musculus* (CAM23928.1); Hs, *Homo sapiens* (NP_919289.2): Tt, *Tetrahymena thermophila* (XP_001026192.1); Lb, *Leishmania braziliensis* (XP_001563287.1). (C) Cartoon graphic and sequence of the orphan kinesin Kif9. The motor domain is in blue; the sequence highlighted in orange indicates the position of a transmembrane domain.

MTOC duplicates during prophase and is brought to or into a fenestration of the nuclear envelope, and then it establishes an intranuclear bipolar spindle for division (39, 53, 64). While MTOCs can be purified from *Dictyostelium*, the methods rely heavily on reagents that actively disrupt the attached nuclei (10, 59). A recent study has identified at least one component of this connection, the nuclear envelope protein Sun-1 (67). The perturbation of Sun-1 affects nuclear shape and results in centrosome detachment, hyperamplification, and aneuploidy. We demonstrate in the current work that the disruption of the Kif9 kinesin also perturbs the MTOC-nucleus linkage. Our results suggest that an MT-mediated mechanism plays a significant role in maintaining an MTOC-nucleus connection during interphase, and we discuss how this connection could be important to regulate centrosome replication and ensure proper chromosome segregation during cell division.

MATERIALS AND METHODS

Molecular genetics. The sequence of the *kif9* gene (DDB0185204) was obtained from http://dictybase.org/. For assembly of the disruption construct, we used the following primer combinations to amplify a 1.2-kb genomic fragment from AX-2 cell DNA: forward, 5′ C**TGAATTC**CCCTACCTCCATCACAACA ATTAAG 3′ (+303 to +332); reverse, 5′ CCG**AAGCTT**ACCCCATGATGAT GGTAATAGTTG 3′ (+1456 to +1480) (+1 indicates the A of the ATG start codon). Restriction enzyme sites were engineered into the ends of each primer (EcoRI and HindIII; shown in boldface in the sequences described above) and used for the cloning of the amplified DNA into pUC19. SwaI and BclI restrictions sites (see Fig. 3) were used to excise and replace a 238-bp internal fragment of the *kif9* sequence (+896 to +1134) with the 1.6-kb blasticidin cassette (*Bsr*′) (SmaI digest) from pLRBLP (8), which was obtained from the *Dictyostelium* Stock Center (http://dictybase.org/StockCenter/StockCenter.html). The *kif9* construct was designed to terminate message coding at H299, a position well upstream from the kinesin motor domain sequence.

The *kif6* long hairpin constructs were assembled with PCR-generated fragments as outlined in Fig. S1 in the supplemental material (9). The initial segment (for *kif6*, bp +1894 to +2445) was amplified with primers containing 5′ NotI and 3′ SalI restriction sites and cloned in reverse orientation relative to the actin-15 promoter in pLD1A15SN (50). The second segment (+2059 to +2445) was amplified with primers containing 5′ NotI and 3′ MluI restriction sites and was cloned downstream but in a forward orientation adjacent to the initial segment. Expression should yield a single RNA transcript that folds into a hairpin, with a large unpaired loop (for *kif6*, 165 bases). An identical strategy was followed for the dynein heavy chain and *kif13* hairpin constructs. For inducible expression, the entire hairpin loop cassette was excised with SalI and MluI digestion and then was blunt/sticky-cloned into BglII/MluI sites in the MB38 plasmid (2).

Standard molecular biology procedures were followed for DNA isolation, manipulation, and blotting. The *kif9* Southern blotting was performed using chemiluminescence procedures (ECL; Amersham Biosciences), and the blot was probed with the initial 1.2-kb amplified genomic target of *kif9*. Quantitative reverse transcription-PCR (RT-PCR) was performed using a LightCycler instrument (Roche Applied Science). DNA-free total RNA was isolated from cells with an RNeasy kit (Qiagen). For each reaction, 1 μg of RNA was transcribed into cDNA (Omniscript RT kit; Qiagen); 1/50 of this product was used for RT-PCR with the SYBR green JumpStart *Taq* ReadyMix kit (Sigma Chemical Co). Primers and conditions were optimized to produce single bands of predicted sizes, amplifying targets of 300 to 400 bp located outside of the conserved motor domains. Primer sequences and PCR conditions are available upon request.

Cell transformation and culture. For homologous recombination, we used a calcium phosphate method to transform *Dictyostelium* AX-2 cells, as described previously (6, 42). The PCR amplification of a 0.9-kb target, with a primer upstream of the recombination site (+53 to +77) (5′ CCCAAGCTTCAACTA CTGGCGGTCAATTAAGGTC 3′) and a primer internal to the *Bsr*′ cassette (5′

GTATGCTATACGAAGTTATCCATGG 3′), was used initially to identify positive recombinants. Clones were further purified by serial dilution, again confirmed by PCR, and tested for proper marker integration by Southern blot analysis.

For hairpin expression, AX-2 or HR38-D2 cells were transformed by electroporation following methods described previously (22). The latter strain contained an integrated copy of the MB35 transactivator plasmid, which is necessary for tetracycline-inducible expression from MB35 plasmid constructs. For growth measurements, room temperature shaking cultures were counted with a hemocytometer at 24-h intervals; growth curves were calculated and displayed with Microsoft Excel.

Light microscopy. Cells were processed for immunofluorescence by following methods described previously (42, 60). Z-series stacks of images were obtained on a DeltaVision microscopy workstation and were deconvolved using softWoRx 2.5 (Applied Precision, Issaquah, WA). Maximum-intensity projections were compiled with ImageJ (NIH); figures were assembled in Adobe Photoshop. Live-cell recordings were performed using wild-type and *kif9*$^-$ cells that had been transformed with a GFP–α-tubulin construct (20, 60). Fluorescence/phase-contrast image pairs were recorded on a Nikon T-300 inverted microscope with a ×100, 1.4-numerical plan apo objective, controlled by IP Lab software (BD Biosciences).

RESULTS

***kif6* and *kif9* each encode a central motor kinesin.** The *kif6* gene encodes a 1,030-amino-acid polypeptide that contains a central motor domain (residues 459 to 776) homologous to members of the kinesin-13 family (Fig. 1A). The motor domain sequence is most similar to the vertebrate KIF24 subfamily, yet it is positioned in the center of the molecule, as is commonly found for KIF2 subfamily members (38). Outside of the motor domain, there are only two short stretches of sequence similar to other kinesin-13 proteins, an amino-terminal domain (*Dd* 8-64) that has homology to a sterile alpha motif (58) and a short carboxy-terminal region (*Dd* 919-976) (Fig. 1B). A striking feature of the Kif6 sequence is the extensive stretches of repeated amide residues (asparagine and glutamine). Together these two amino acids account for 29% of the Kif6 polypeptide (37% total outside of the motor domain), including a 37-residue stretch of asparagines and a region where 44 of 51 residues are glutamines. *Dictyostelium* polypeptides are notably rich in homopolymer tracts of these two amino acids, and thus the repetitions noted in Kif6 are unlikely to be a product of sequencing or annotation errors (7). In fact, the Kif6 sequence outside of the repetitive tracts may be particularly useful in defining key functional domains of other kinesin-13 motors. The *kif9* kinesin also contains a central motor domain (residues 356 to 720, out of 1,222) (Fig. 1C). However, unlike the other 12 *Dictyostelium* kinesin motors, Kif9 does not group with previously recognized kinesin families (38). On the carboxy-terminal side of the motor domain, there is a region predicted to form an alpha-helical coiled-coil domain as well as a transmembrane domain (residues 1182 to 1204) that may be significant in forming motor-to-cargo linkages.

***kif6* is an essential *Dictyostelium* gene.** We screened *Dictyostelium* AX-2 cells with a collection of kinesin RNA interference (RNAi) constructs and found that the targeting of the *kif6* RNA was particularly effective in blocking cell growth. Long hairpin RNAi (lhp) constructs were assembled from PCR-generated fragments by following the strategy depicted in Fig. S1 in the supplemental material (9, 36). These constructs were cloned into the pLD1A15SN plasmid (50), where the robust, constitutively active actin-15 promoter would drive their expression. In none of the multiple transformation attempts with the *kif6* lhp construct did we recover any viable colonies of cells. As controls, we also used lhp constructs for the dynein heavy chain and the kinesin-5 family member *kif13*. Dynein is an essential protein in *Dictyostelium* (27, 34), while *kif13* can be deleted without a significant growth penalty (60). The transformation of AX-2 cells with a similarly designed dynein lhp (see Fig. S1 in the supplemental material) produced the same lethal result (i.e., no viable colonies) as the *kif6* constructs, whereas transformation with the *kif13* lhp routinely produced dozens of viable colonies per 10-cm dish. These results suggest that the expression of the *kif6* lhp is lethal in *Dictyostelium*.

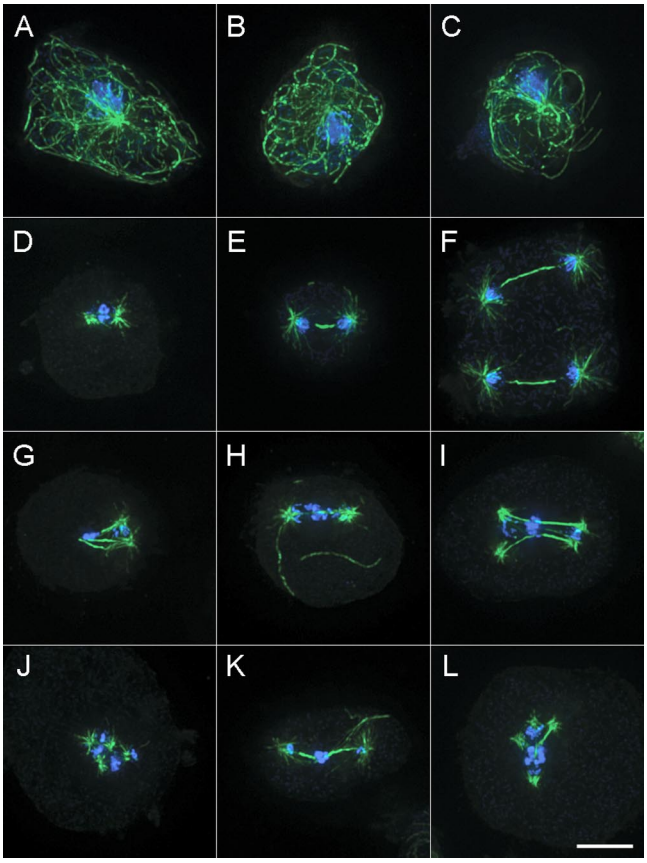

FIG. 2. MT arrays in *kif6* lhp cells. (A to C) Representative interphase wild-type (A) and *kif6* lhp cells (B and C). There are no obvious differences in MT or chromatin patterns. (D to L) Mitotic figures in *kif6* lhp cells. Panels D to F show normal-appearance mitotic spindles in metaphase (D), late anaphase (E), and late telophase (F) (a binucleate cell). (G to L) Aberrant spindle formations due to Kif6 knockdown. (G and J) Malformed metaphase arrangements; (H and K) lagging chromosomes and extracytoplasmic MTs in late anaphase; (I and L) abnormal binucleate spindle and chromatin figures in late telophase. MTs are in green, DNA is in blue. Scale bar = 5 μm.

Since *Dictyostelium* transfection is not particularly efficient, it is not possible to examine individual cells that are transformed with the *kif6* lhp and potentially are dying, against a background of 10^4 to 10^6 nontransformed cells that are sensitive to the G418 antibiotic. As an alternative strategy, we utilized the same *kif6* and *kif13* lhp constructs in the tetracycline-regulated tetOFF plasmid MB38 (2). By waiting 24 h posttransfection before removing tetracycline and inducing *kif6* lhp expression, we were able to recover multiple colonies

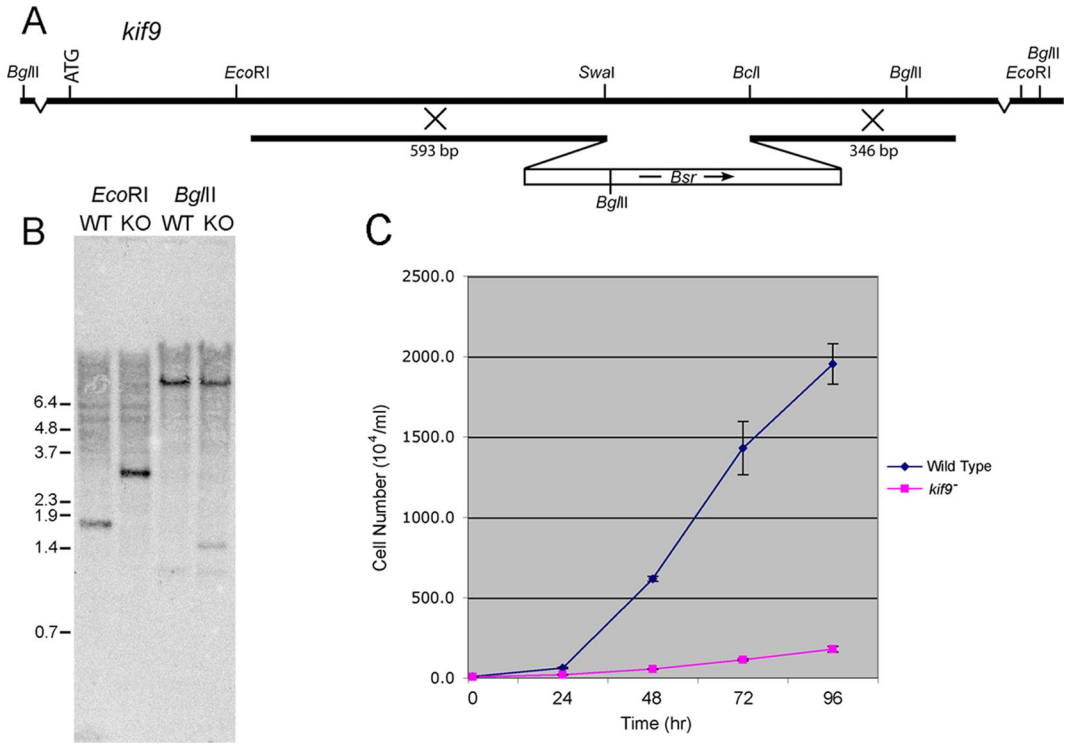

FIG. 3. Gene knockout (KO) of *kif9*. (A) Schematic representation of a recombination construct designed to integrate into the *kif9* locus and disrupt expression. (B) Southern analysis of wild-type (WT) and *kif9*$^-$ transformant DNA. Fragment mass shift in an EcoRI digest (1.7 to 3.1 kb) and the appearance of a new, 1.5-kb band in a BglII digest are exactly as predicted for marker insertion (see panel A). To reduce congestion, only a partial listing of the Lambda DNA-BstEII mass markers are shown. (C) Growth of *kif9*$^-$ cells, demonstrating a substantially reduced rate compared to that of wild-type cells. Error bars indicate standard deviations.

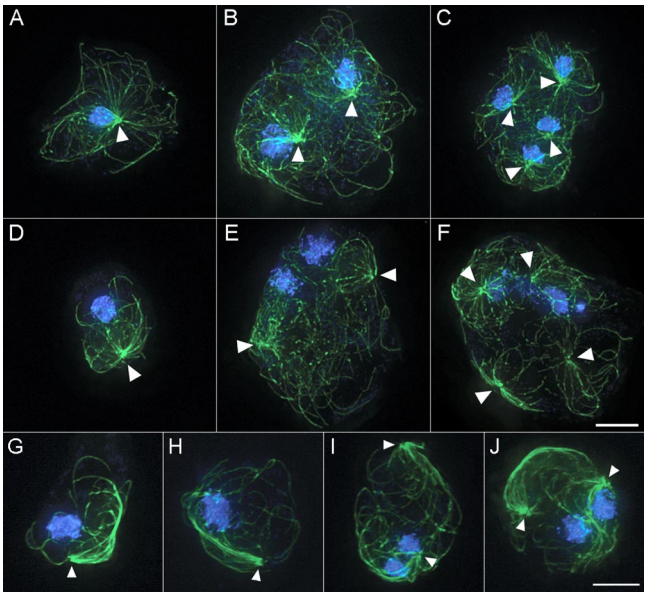

FIG. 4. *kif9* knockout decouples MTOCs from nuclei. (A to C) Three examples of wild-type interphase cells that show the typical tight association between the MTOC (marked with arrowheads) and nucleus. (A) Mononucleate cell with a single MTOC; (B) binucleate cell with two MTOCs; (C) tetranucleate cell with four MTOCs. (D to F) Similar mono-, bi-, and tetranucleate *kif9*$^-$ cells. Most MTOCs appear spatially separated from the nucleus. (G to J) Mono- and binucleate *kif9*$^-$ cells overexpressing the dynein motor domain. Note the characteristic comet-like appearance of the motile MT array and the enhanced separation between the nuclei and MTOCs. MTs are in green, DNA is in blue. Scale bars = 5 μm.

of viable *kif6* lhp cells. However, these cells grow poorly. Under the same conditions, there were ~10-fold more colonies formed on *kif13* lhp control dishes than on the *kif6* lhp dishes. After 1 week in the absence of tetracycline, the *kif13* lhp dishes were confluent, while the *kif6* transformants covered only 10 to 20% of the dish surface. The two cell strains grew equally well in the continued presence of tetracycline, indicating that *kif6* lhp expression negatively affects cell growth. To demonstrate that the *kif6* lhp was effective in reducing endogenous levels of *kif6* mRNA, we measured message levels in cells using quantitative RT-PCR. Cells were transfected with the *kif6* lhp and grown to near confluence in the presence of tetracycline. At this point, cells were washed free of tetracycline to induce hairpin expression. After 19 h of induction, the *kif6* lhp cell population showed a 50% reduction in *kif6* mRNA relative to wild-type levels in control (MB35) cells (data not shown). This result indicates that the *kif6* lhp construct does function to reduce the level of endogenous message and therefore is likely to negatively affect Kif6 protein functioning.

We further examined MT arrays in the *kif6* lhp cells. While

TABLE 1. Percentages of mono- and multinucleated cells

Cell type	% Mononucleate	% Binucleate	% Trinucleate	Other (%)	Total no. of cells
Wild type	64	26	6	4	150
kif9$^-$	66	22	6	6	167

TABLE 2. Number of MTOCs in mono- and multinucleate cells

No. of MTOCs	No. of cells					
	Mononucleate		Binucleate		Trinucleate	
	Wild type	*kif9*$^-$	Wild type	*kif9*$^-$	Wild type	*kif9*$^-$
1	96	106	1	7	0	0
2	0	4	38	24	0	0
3	0	0	0	5	9	6
4	0	0	0	1	0	4

interphase MT arrays appeared identical to those found in wild-type cells, significant defects were evident in mitotic spindle assemblies in the *kif6* lhp cells (Fig. 2). Examples of spindle malformations include aberrant MT arrangements, extra spindle MTs, and, in particular, lagging chromosomes during anaphase/telophase. In total, obvious defects were found in 38% (26/68) of the mitotic *kif6* lhp cells; 62% of the cells had normal-appearing mitotic figures. This difference likely reflects the known variations in individual cell expression levels for this promoter sequence (2). None of the aberrant spindle morphologies were seen in wild-type AX-2 cells, and they are consistent with the defects described for the kinesin-13 family of motors in vertebrate cells. Thus, these data, taken together, indicate that Kif6 should be considered essential for viability in *Dictyostelium*, and that its function contributes to proper chromosome segregation and mitotic spindle organization.

***kif9* participates in the nucleus-MTOC connection.** We constructed a plasmid to introduce a deletion-disruption allele of *kif9* into the AX-2 cell genome (Fig. 3A). After transformation, individual *Bsr*^{r} colonies were tested by PCR to identify clones containing the predicted marker insertion, and these clones were further confirmed by Southern hybridization (Fig. 3B) and RNA analyses (not shown). There were no obvious morphological differences in cell shape or size between *kif9*$^-$ and wild-type cells, and *kif9*$^-$ cells were able to complete a full developmental cycle to generate viable spores. However, the *kif9* disruption resulted in significantly reduced growth rates (Fig. 3C).

A closer examination of the MT array revealed a striking difference from wild-type cells. In wild-type cells, the MTOC is tightly associated with the nucleus; by our light microscopy analysis, 97% of MTOCs were found within a 1-μm distance of the nucleus (118/122 nuclei; also see reference 39). MTOCs are further maintained at a strict 1:1 MTOC/nucleus ratio, even in multinucleated cells (Fig. 4A to C; Tables 1 and 2). In the absence of Kif9, the MTOC could be found spatially separated from the nucleus (Fig. 4D to F). The extent of separation was variable; occasionally the nuclei and MTOCs were found on opposite sides of the cytoplasm. Forty-nine percent of the MTOCs in *kif9*$^-$ cells (71/146 nuclei) were greater than 1 μm distant from the nucleus. This separation was further accentuated in *kif9*$^-$ cells that contain excess dynein motor (Fig. 4G to J), a dominant-negative effect that stimulates MTOC movement through the cytoplasm (28).

In terms of MT number, length, and arrangement, the interphase MT network in *kif9*$^-$ cells otherwise appeared identical to wild-type cells, indicating that MT nucleation is not affected by the loss of Kif9. However, the *kif9*$^-$ cells showed further variability in the nucleus/MTOC ratio (Tables 1 and 2). While 99% of wild-type cells contained a single MTOC-nuclei pair, >13% of *kif9*$^-$ cells contained an abnormal ratio; for example, binucleate cells contained from 1 to 4 distinct organizing centers (Tables 1 and 2). Using a Fisher's exact test (a two-by-two contingency table), the two-tailed *P* values for both the MTOC-nuclear separation data and MTOC number per nuclei were 0.0001, indicating that these differences between *kif9*-null and wild-type cells are statistically significant. These results suggest that Kif9 not only functions in maintaining a close physical connection between the nucleus and MTOC in interphase cells but also that this connection is important in the strict control of the number of MTOCs present in the cytoplasm.

The imaging of live *kif9*$^-$ cells transformed with a GFP-tubulin expression construct revealed a dynamic association of the MTOC with the nucleus during interphase (Fig. 5). As in wild-type cells, examples could be found with the MTOC sufficiently tethered to the nucleus to produce nuclear distortion upon MTOC movement. Other cells showed no obvious connection between the MTOC and nucleus. In these cases, the MTOC underwent transient back-and-forth motions, but there were no corresponding shape changes or movement of the

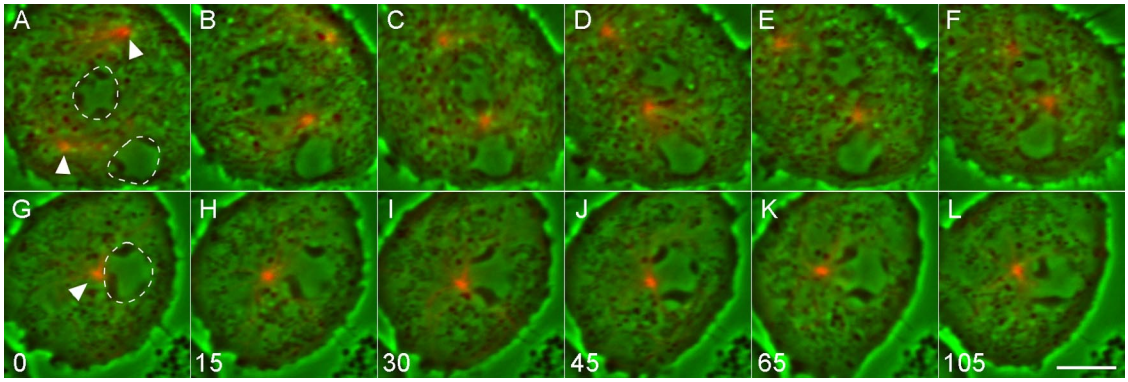

FIG. 5. MTOC-nucleus connection in live cells. (A to F) Sequence of a binucleate *kif9*$^-$ cell with two MTOCs, in which the movements of the MTOCs appear independent of the nuclei. (G to L) Control panel showing the close apposition of a single MTOC with the nucleus during identical time frames. Nuclei are outlined in white, and the GFP-labeled MTOCs are highlighted with arrowheads in panels A and G. Time is in seconds. Scale bar = 5 μm.

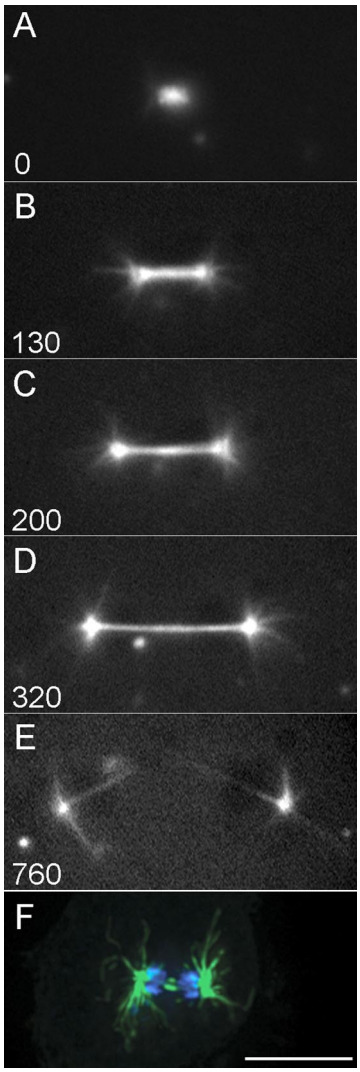

FIG. 6. Mitotic progression in *kif9*$^-$ cells. (A to E) Sequence following a live, GFP-tubulin-labeled *kif9*$^-$ cell as it progresses through karyokinesis. Spindle assembly and elongation appear normal. (F) Image of a different, fixed *kif9*$^-$ cell stained with a tubulin antibody/Hoechst in mid-late anaphase showing the complete segregation of chromatin to the two spindle poles (a stage roughly equivalent to the frame shown in panel B). Time is in seconds. Scale bar = 5 μm.

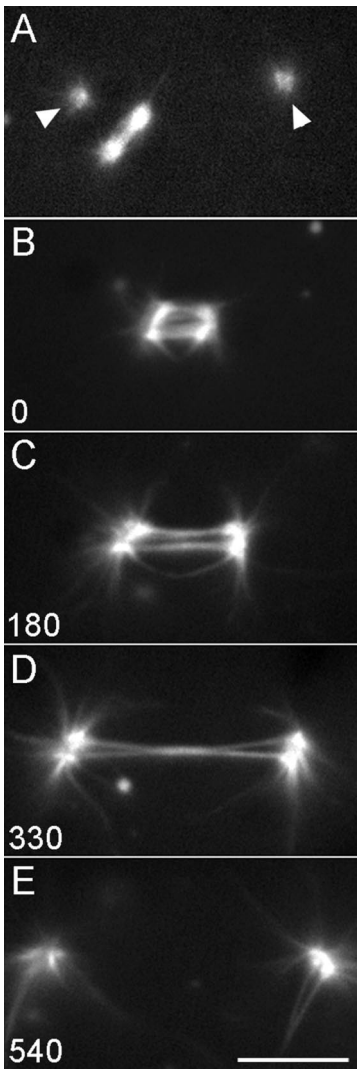

FIG. 7. Mitotic anomalies in *kif9*$^-$ cells. (A) Frame from a live *kif9*$^-$ cell sequence showing a normal bipolar spindle (center) flanked by two additional cytoplasmic MTOCs (arrowheads). Note that the MTOCs are associated with a few short MTs, similarly to the cytoplasmic face of the spindle poles. (B to E) Sequence of a different *kif9*$^-$ cell showing a double spindle as it proceeds though division. Time is in seconds. Scale bar = 5 μm.

nuclear envelope to indicate linkage. We could discern a number of intermediate cases where the MTOC appeared to attach and detach from the nucleus or where a single MTOC appeared to associate with more than one nucleus in a multinucleated cell. These examples further support the role of Kif9 in maintaining a connection between the MTOC and nucleus but also demonstrate that Kif9 is not the sole means of attachment.

Mitotic spindle elongation appears normal in *kif9*$^-$ cells. We monitored the spindle assembly process in *kif9*$^-$/GFP-tubulin cells. In all cases (12/12) where a bipolar spindle was observed, the spindle continued on through division in a manner indistinguishable from the process in wild-type cells (Fig. 6). Spindle elongation proceeded at a rate of 2.1 ± 0.5 μm/min and achieved an average length of 11.0 μm before breakage (n = 6) (wild-type spindles elongate at 1.6 ± 0.2 μm/min and attain a length of 10.9 μm; these data were taken from reference 60). In no case was there any evidence for lagging chromosomes, a phenomenon observed in knockdowns of the other central motor kinesin, Kif6. This result indicates that Kif9 does not play a significant role in spindle elongation or function.

However, there were a few interesting observations during the earliest stages of mitosis. We viewed a number of cells with supernumerary MTOCs entering mitosis (n = 10). In these cells, all of the MTOCs had lost their cytoplasmic MTs, but only those MTOCs that appeared properly associated with the nucleus went on to develop a bipolar spindle (Fig. 7). Second, we also found a couple of double-spindle arrangements. Multiple MTOCs appear to have been tethered to the nucleus upon mitosis; at least two in Fig. 7 appear to have duplicated

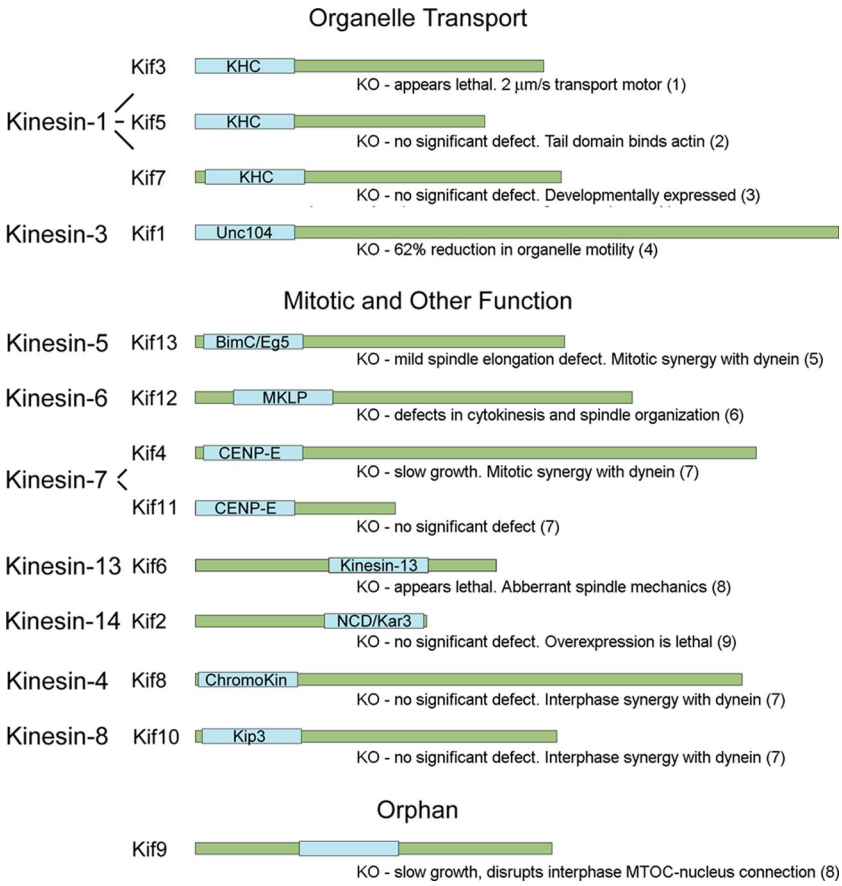

FIG. 8. Summary of the kinesin motor family in *Dictyostelium*. For each kinesin, the motor domains are shown in blue, and the green represents flanking neck and tail domains (drawn to scale). KO, knockout. Numbers in parentheses reference the following texts: 1, reference 51; 2, 17; 3, 5; 4, 46; 5, 60; 6, 30; 7, 42; 8, data presented in this paper; 9, 18. This figure was inspired from reference 24 and adapted with permission from reference 42.

and assembled independent spindles. This result suggests that there are multiple MTOC docking sites on the nucleus. Finally, despite the consequent strong growth defect and potential for multipolar divisions, the *kif9* deletion did not appear to increase the ploidy of cells. The percentages of single-, bi-, and tri-nucleate cells in the *kif9*$^-$ population remain unchanged from the proportions seen in wild-type cells (Tables 1 and 2).

DISCUSSION

We have individually disrupted functions of the two central motor kinesins in *Dictyostelium* and have shown here that they participate in independent MT-nuclear-based processes. Kif6 (of the kinesin-13 family) appears essential for viability, with a role in chromosome segregation during cell division; Kif9 (an orphan) participates in maintaining a connection between the MTOC and nucleus during interphase. On a broader scale, the present work completes a survey of the individual kinesin motor actions in *Dictyostelium*, as summarized in Fig. 8.

Eight *Dictyostelium* kinesins (Kif2, Kif4, Kif6, Kif8, Kif10, Kif11, Kif12, and Kif13) contain sequence homology with families known to participate in at least some aspect of cell division (24). However, only Kif6 appears to be absolutely required for mitosis (18, 30, 42, 60). The defects seen here in *kif6* lhp cells (lagging chromosomes, malformed spindles, and extraneous cytoplasmic MTs) are very similar to phenotypes associated with disruptions of kinesin-13 motors in other organisms (40), indicating a likely role in coordinating kinetochore-MT attachments and spindle MT depolymerization. Defects associated with *kif12* (encoding the kinesin-6 isoform of the MKLP family) knockout in *Dictyostelium* (such as cytokinesis and spindle assembly defects) (30) also are comparable with this motor's known biological activities in other systems (see, e.g., reference 37). Thus, kinesin-13 and kinesin-6 isoforms appear to perform similar functions in a wide range of organisms and diverse spindle configurations. However, in contrast to their essential roles in vertebrate cells (19, 45, 47, 65), Kif13 (the kinesin-5 isoform of the BimC/Eg5 family), Kif4 (the kinesin-7 isoform of the CENP-E family), and Kif2 (the kinesin-14 isoform of the NCD/Kar3 family) are not strictly required for division in *Dictyostelium*. In addition, there are no obvious mitotic defects in knockouts of the other three kinesins, Kif8 (the kinesin-4 isoform of the chromokinesin family), Kif10 (the kinesin-8 isoform of the Kip3 family), and Kif11 (a truncated kinesin-7 family member) (42). Thus, the relatively small, compact intranuclear spindle of *Dictyostelium* offers an opportune model to compare and contrast the evolution of essential mitotic motor activities.

The second central motor kinesin in *Dictyostelium*, Kif9 (orphan), functions in a nuclear role completely separate from that of Kif6, to form at least part of the linkage between the interphase nucleus and the MTOC. Previous structural studies have described 4- to 5-nm-diameter fibers connecting the centrosome and nuclear envelope, and the tight linkage between these two objects is maintained even in the presence of MT poisons (29, 44). Thus, it is unlikely that the MT system comprises the sole physical connection between the nucleus and MTOC. However, several interesting observations can be made here. Live-cell imaging indicates that in the absence of Kif9, the nucleus-MTOC connection is dynamic: MTOCs are seen either closely tethered to or spatially separated from the nucleus, and they appear to attach and detach from this organelle. Thus, at one level, the Kif9 activity appears to reinforce a tether already formed through another mechanism. Sun-1 recently has been identified in *Dictyostelium* (67) as an inner nuclear membrane component of the KASH/SUN pathway of transnuclear linkers (21, 57, 62). The reduced activity of Sun-1 through dominant-negative fragment expression or RNAi produces defects similar to the deletion of Kif9, namely centrosome-nuclear separation and centrosome hyperamplification. Efforts currently are under way to determine whether Kif9 operates in the same pathway as Sun-1 or whether it defines a completely independent mechanism of anchoring the MTOC to the nucleus. A plausible mechanism of action for Kif9 involves a central motor MT depolymerase activity. If Kif9 functions similarly to MCAK-type kinesins (41), then it should bind MTs, effect plus-end depolymerization, and thus processively move toward the MTOC. If Kif9 were connected to the nucleus, the MT depolymerization activity would provide a constant traction force to keep the nucleus closely apposed to the MTOC. We are working to test this idea to address whether Kif9 moves along or depolymerizes MTs, as well as to determine the function of the protein's carboxy-terminal transmembrane domain.

In maintaining a nucleus-MTOC connection during interphase, Kif9 has a function thus far undescribed for kinesin motors. It could be argued that because of Kif9's orphan status, this protein's function is important only in organisms with similar close linkages between the nucleus and MTOC (11, 12, 52). However, even in vertebrate cells, the centrosome/MTOC is not completely independent of the nucleus, and motors such as dynein have been implicated in nuclear motility and envelope disruption in a number of different organisms (1, 31, 35, 55, 61, 66). Our work could further point toward a general requirement of multiple motor interactions that link nuclei and MTOCs. We suggest that Kif9 plays a role in the transition from interphase to mitosis. Upon entry into mitosis, the MTOC must be positioned into the nucleus for spindle assembly. Movement driven by Brownian motion and guided by fibrous tethers may indirectly dock the centrosome into the nucleus, a mechanism that would account for some cell growth in the absence of Kif9. However, a dedicated motor activity that pulls the MTOC into the nucleus would significantly increase the fidelity of this process, ensuring centrosome duplication and spindle assembly in the proper nuclear environment. We are currently testing this hypothesis.

ACKNOWLEDGMENTS

We are grateful to the dictyBase team (http://dictybase.org) in archiving and annotating *Dictyostelium* sequence information and to the *Dictyostelium* Stock Center Resource for plasmids. Susan Wu and Erasmus Schneider patiently answered our endless questions about real-time PCR and provided the generous use of their equipment for these assays. Alexey Khodjakov and Conly Rieder provided valuable discussion and assistance with the light microscopy. We acknowledge the use of the Wadsworth Center's Molecular Genetics Core for DNA sequencing.

This work was supported in part by the NSF (MCB-0542731 to M.P.K.) and the NIH (GM066817 to D.N.R.).

REFERENCES

1. **Beaudouin, J., D. Gerlich, N. Daigle, R. Eils, and J. Ellenberg.** 2002. Nuclear envelope breakdown proceeds by microtubule-induced tearing of the lamina. Cell **108:**83–96.
2. **Blaauw, M., M. H. K. Linskens, and P. J. M. van Haastert.** 2000. Efficient control of gene expression by a tetracycline-dependent transactivator in single *Dictyostelium discoideum* cells. Gene **252:**71–82.
3. **Blaineau, C., M. Tessier, P. Dubessay, L. Tasse, L. Crobu, M. Pages, and P. Bastien.** 2007. A novel microtubule-depolymerizing kinesin involved in length control of a eukaryotic flagellum. Curr. Biol. **17:**778–782.
4. **Dawson, S. C., M. S. Sagolla, J. J. Mancuso, D. J. Woessner, S. A. House, L. Fritz-Laylin, and W. Z. Cande.** 2007. Kinesin-13 regulates flagellar, interphase, and mitotic microtubule dynamics in *Giardia intestinalis*. Eukaryot. Cell **6:**2354–2364.
5. **de Hostos, E. L., G. McCaffrey, R. Sucgang, D. W. Pierce, and R. D. Vale.** 1998. A developmentally regulated kinesin-related motor protein from *Dictyostelium discoideum*. Mol. Biol. Cell **9:**2093–2106.
6. **Egelhoff, T. T., M. A. Titus, D. J. Manstein, K. M. Ruppel, and J. A. Spudich.** 1991. Molecular genetic tools for study of the cytoskeleton in *Dictyostelium*, p. 319–334. *In* R. B. Vallee (ed.), Methods in enzymology, vol. 196. Academic Press, New York, NY.
7. **Eichinger, L., J. A. Pachebat, G. Glockner, M. A. Rajandream, R. Sucgang, M. Berriman, J. Song, R. Olsen, K. Szafranski, Q. Xu, B. Tunggal, S. Kummerfeld, M. Madera, B. A. Konfortov, F. Rivero, A. T. Bankier, R. Lehmann, N. Hamlin, R. Davies, P. Gaudet, P. Fey, K. Pilcher, G. Chen, D. Saunders, E. Sodergren, P. Davis, A. Kerhornou, X. Nie, N. Hall, C. Anjard, L. Hemphill, N. Bason, P. Farbrother, B. Desany, E. Just, T. Morio, R. Rost, C. Churcher, J. Cooper, S. Haydock, N. van Driessche, A. Cronin, I. Goodhead, D. Muzny, T. Mourier, A. Pain, M. Lu, D. Harper, R. Lindsay, H. Hauser, K. James, M. Quiles, M. Madan Babu, T. Saito, C. Buchrieser, A. Wardroper, M. Felder, M. Thangavelu, D. Johnson, A. Knights, H. Loulseged, K. Mungall, K. Oliver, C. Price, M. A. Quail, H. Urushihara, J. Hernandez, E. Rabbinowitsch, D. Steffen, M. Sanders, J. Ma, Y. Kohara, S. Sharp, M. Simmonds, S. Spiegler, A. Tivey, S. Sugano, B. White, D. Walker, J. Woodward, T. Winckler, Y. Tanaka, G. Shaulsky, M. Schleicher, G. Weinstock, A. Rosenthal, E. C. Cox, R. L. Chisholm, R. Gibbs, W. F. Loomis, M. Platzer, R. R. Kay, J. Williams, P. H. Dear, A. A. Noegel, B. Barrell, and A. Kuspa.** 2005. The genome of the social amoeba *Dictyostelium discoideum*. Nature **435:**43–57.
8. **Faix, J., L. Kreppel, G. Shaulsky, M. Schleicher, and A. R. Kimmel.** 2004. A rapid and efficient method to generate multiple gene disruptions in *Dictyostelium discoideum* using a single selectable marker and the Cre-loxP system. Nucleic Acids Res. **32:**e143.
9. **Girard, K. D., C. Chaney, M. Delannoy, S. C. Kuo, and D. N. Robinson.** 2004. Dynacortin contributes to cortical viscoelasticity and helps define the shape changes of cytokinesis. EMBO J. **23:**1536–1546.
10. **Gräf, R., U. Euteneuer, M. Ueda, and M. Schliwa.** 1998. Isolation of nucleation-competent centrosomes from *Dictyostelium discoideum*. Eur. J. Cell Biol. **76:**167–175.
11. **Guhl, B., and U.-P. Roos.** 1994. Microtubule centers and the interphase microtubule cytoskeleton in amoebae of the cellular slime molds (mycetozoans) *Acytostelium leptosomum* and *Protostelium mycophaga*. Cell Motil. Cytoskel. **28:**45–58.
12. **Heath, I. B.** 1981. Nucleus-associated organelles in fungi. Int. Rev. Cytol. **69:**191–221.
13. **Hertzer, K. M., S. C. Ems-McClung, and C. E. Walczak.** 2003. Kin I kinesins: insights into the mechanism of depolymerization. Critical Rev. Biochem. Mol. Biol. **38:**453–469.
14. **Hildebrandt, E. R., and M. A. Hoyt.** 2000. Mitotic motors in *Saccharomyces cerevisiae*. Biochim. Biophys. Acta Mol. Cell Res. **1496:**99–116.
15. **Homma, N., Y. Takei, Y. Tanaka, T. Nakata, S. Terada, M. Kikkawa, Y. Noda, and N. Hirokawa.** 2003. Kinesin superfamily protein 2A (KIF2A) functions in suppression of collateral branch extension. Cell **114:**229–239.
16. **Howard, J., and A. A. Hyman.** 2007. Microtubule polymerases and depolymerases. Curr. Opin. Cell Biol. **19:**31–35.
17. **Iwai, S., A. Ishiji, I. Mabuchi, and K. Sutoh.** 2004. A novel actin-bundling

kinesin-related protein from Dictyostelium discoideum. J. Biol. Chem. **279:** 4696–4704.
18. **Iwai, S., E. Suyama, H. Adachi, and K. Sutoh.** 2000. Characterization of a C-terminal-type kinesin-related protein from *Dictyostelium discoideum*. FEBS Lett. **475:**47–51.
19. **Kashina, A. S., G. C. Rogers, and J. M. Scholey.** 1997. The bimC family of kinesins: essential bipolar mitotic motors driving centrosome separation. Biochim. Biophys. Acta Mol. Cell Res. **1357:**257–271.
20. **Kimble, M., C. Kuzmiak, K. N. McGovern, and E. L. de Hostos.** 2000. Microtubule organization and the effects of GFP-tubulin expression in *Dictyostelium discoideum*. Cell Motil. Cytoskel. **47:**48–62.
21. **King, M. C., T. G. Drivas, and G. Blobel.** 2008. A network of nuclear envelope membrane proteins linking centromeres to microtubules. Cell **134:** 427–438.
22. **Knecht, D. A., J. Jung, and L. Matthews.** 1990. Quantification of transformation efficiency using a new method for clonal growth and selection of axenic *Dictyostelium* cells. Dev. Genet. **11:**403–409.
23. **Kollmar, M.** 2006. Thirteen is enough: the myosins of *Dictyostelium discoideum* and their light chains. BMC Genomics **7:**183.
24. **Kollmar, M., and G. Glockner.** 2003. Identification and phylogenetic analysis of *Dictyostelium discoideum* kinesin proteins. BMC Genomics **4:**47.
25. **Koonce, M. P.** 2000. *Dictyostelium*, a model organism for microtubule-based transport. Protist **151:**17–25.
26. **Koonce, M. P., P. M. Grissom, and J. R. McIntosh.** 1992. Dynein from *Dictyostelium*: primary structure comparisons between a cytoplasmic motor enzyme and flagellar dynein. J. Cell Biol. **119:**1597–1604.
27. **Koonce, M. P., and D. A. Knecht.** 1998. Cytoplasmic dynein heavy chain is an essential gene product in *Dictyostelium*. Cell Motil. Cytoskel. **39:**63–72.
28. **Koonce, M. P., J. Kohler, R. Neujahr, J. M. Schwartz, I. Tikhonenko, and G. Gerisch.** 1999. Dynein motor regulation stabilizes interphase microtubule arrays and determines centrosome position. EMBO J. **18:**6786–6792.
29. **Kuriyama, R., C. Sato, Y. Fukui, and S. Nishibayashi.** 1982. In vitro nucleation of microtubules from microtubule-organizing center prepared from cellular slime mold. Cell Motil. Cytoskel. **2:**257–272.
30. **Lakshmikanth, G. S., H. M. Warrick, and J. A. Spudich.** 2004. A mitotic kinesin-like protein required for normal karyokinesis, myosin localization to the furrow, and cytokinesis in *Dictyostelium*. Proc. Natl. Acad. Sci. USA **101:**16519–16524.
31. **Levy, J. R., and E. L. F. Holzbaur.** 2008. Dynein drives nuclear rotation during forward progression of motile fibroblasts. J. Cell Sci. **121:**3187–3195.
32. **Lu, L., Y.-R. J. Lee, R. Pan, J. N. Maloof, and B. Liu.** 2005. An internal motor kinesin is associated with the Golgi apparatus and plays a role in trichome morphogenesis in *Arabidopsis*. Mol. Biol. Cell **16:**811–823.
33. **Ma, S., and R. L. Chisholm.** 2002. Cytoplasmic dynein-associated structures move bidirectionally in vivo. J. Cell Sci. **115:**1453–1460.
34. **Ma, S., L. Trivinos-Lagos, R. Graf, and R. L. Chisholm.** 1999. Dynein intermediate chain mediated dynein-dynactin interaction is required for interphase microtubule organization and centrosome replication and separation in *Dictyostelium*. J. Cell Biol. **147:**1261–1274.
35. **Malone, C. J., L. Misner, N. Le Bot, M.-C. Tsai, J. M. Campbell, J. Ahringer, and J. G. White.** 2003. The *C. elegans* hook protein, ZYG-12, mediates the essential attachment between the centrosome and nucleus. Cell **115:**825–836.
36. **Martens, H., J. Novotny, J. Oberstrass, T. L. Steck, P. Postlethwait, and W. Nellen.** 2002. RNAi in *Dictyostelium*: the role of RNA-directed RNA polymerases and double-stranded RNase. Mol. Biol. Cell **13:**445–453.
37. **Matuliene, J., and R. Kuriyama.** 2002. Kinesin-like protein CHO1 is required for the formation of midbody matrix and the completion of cytokinesis in mammalian cells. Mol. Biol. Cell **13:**1832–1845.
38. **Miki, H., Y. Okada, and N. Hirokawa.** 2005. Analysis of the kinesin superfamily: insights into structure and function. Trends Cell Biol. **15:**467–476.
39. **Moens, P. B.** 1976. Spindle and kinetochore morphology of *Dictyostelium discoideum*. J. Cell Biol. **68:**113–122.
40. **Moore, A., and L. Wordeman.** 2004. The mechanism, function and regulation of depolymerizing kinesins during mitosis. Trends Cell Biol. **14:**537–546.
41. **Moores, C. A., and R. A. Milligan.** 2006. Lucky 13—microtubule depolymerisation by kinesin-13 motors. J. Cell Sci. **119:**3905–3913.
42. **Nag, D. K., I. Tikhonenko, I. Soga, and M. P. Koonce.** 2008. Disruption of four kinesin genes in *Dictyostelium*. BMC Cell Biol. **9:**21.
43. **Noda, Y., R. Sato-Yoshitake, S. Kondo, M. Nangaku, and N. Hirokawa.** 1995. KIF2 is a new microtubule-based anterograde motor that transports membranous organelles distinct from those carried by kinesin heavy chain or KIF3A/B. J. Cell Biol. **129:**157–167.
44. **Omura, F., and Y. Fukui.** 1985. *Dictyostelium* MTOC: structure and linkage to the nucleus. Protoplasma **127:**212–221.
45. **Ovechkina, Y., and L. Wordeman.** 2003. Unconventional motoring: an overview of the Kin C and Kin I kinesins. Traffic **4:**367–375.
46. **Pollock, N., E. L. de Hostos, C. W. Turck, and R. D. Vale.** 1999. Reconstitution of membrane transport powered by a novel dimeric kinesin motor of the Unc104/KIF1A family purified from *Dictyostelium*. J. Cell Biol. **147:**493–506.
47. **Putkey, F. R., T. Cramer, M. K. Morphew, A. D. Silk, R. S. Johnson, J. R. McIntosh, and D. W. Cleveland.** 2002. Unstable kinetochore-microtubule capture and chromosomal instability following deletion of CENP-E. Dev. Cell **3:**351–365.
48. **Rehberg, M., and R. Graf.** 2002. *Dictyostelium* EB1 is a genuine centrosomal component required for proper spindle formation. Mol. Biol. Cell **13:**2301–2310.
49. **Rehberg, M., J. Kleylein-Sohn, J. Faix, T. H. Ho, I. Schulz, and R. Graf.** 2005. *Dictyostelium* LIS1 is a centrosomal protein required for microtubule/cell cortex interactions, nucleus/centrosome linkage, and actin dynamics. Mol. Biol. Cell **16:**2759–2771.
50. **Robinson, D. N., and J. A. Spudich.** 2000. Dynacortin, a genetic link between equatorial contractility and global shape control discovered by library complementation of a *Dictyostelium discoideum* cytokinesis mutant. J. Cell Biol. **150:**823–838.
51. **Röhlk, C., M. Rohlfs, S. Leier, M. Schliwa, X. Liu, J. Parsch, and G. Woehlke.** 2008. Properties of the kinesin-1 motor DdKif3 from *Dictyostelium discoideum*. Eur. J. Cell Biol. **87:**237–249.
52. **Roos, U. P.** 1975. Fine structure of an organelle associated with the nucleus and cytoplasmic microtubules in the cellular slime mould *Polysphondylium violaceum*. J. Cell Sci. **18:**315–326.
53. **Roos, U. P., and R. Camenzind.** 1981. Spindle dynamics during mitosis in *Dictyostelium discoideum*. Eur. J. Cell Biol. **25:**248–257.
54. **Roos, U. P., M. DeBrabander, and R. Nuydens.** 1987. Movements of intracellular particles in undifferentiated amebae of *Dictyostelium discoideum*. Cell Motil. Cytoskel. **7:**258–271.
55. **Salina, D., K. Bodoor, D. M. Eckley, T. A. Schroer, J. B. Rattner, and B. Burke.** 2002. Cytoplasmic dynein as a facilitator of nuclear envelope breakdown. Cell **108:**97–107.
56. **Santama, N., J. Krijnse-Locker, G. Griffiths, Y. Noda, N. Hirokawa, and C. G. Dotti.** 1998. KIF2beta, a new kinesin superfamily protein in non-neuronal cells, is associated with lysosomes and may be implicated in their centrifugal translocation. EMBO J. **17:**5855–5867.
57. **Schneider, M., A. A. Noegel, and I. Karakesisoglou.** 2008. KASH-domain proteins and the cytoskeletal landscapes of the nuclear envelope. Biochem. Soc. Trans. **36:**1368–1372.
58. **Schultz, J., C. P. Ponting, K. Hofmann, and P. Bork.** 1997. SAM as a protein interaction domain involved in developmental regulation. Protein Sci. **6:**249–253.
59. **Schulz, I., Y. Reinders, A. Sickmann, and R. Gräf.** 2006. An improved method for *Dictyostelium* centrosome isolation. Methods Mol. Biol. **346:**479–489.
60. **Tikhonenko, I., D. K. Nag, N. Martin, and M. P. Koonce.** 2008. Kinesin-5 is not essential for mitotic spindle elongation in *Dictyostelium*. Cell Motil. Cytoskel. **65:**853–862.
61. **Tsai, J.-W., K. H. Bremner, and R. B. Vallee.** 2007. Dual subcellular roles for LIS1 and dynein in radial neuronal migration in live brain tissue. Nat. Neurosci. **10:**970–979.
62. **Tzur, Y. B., K. L. Wilson, and Y. Gruenbaum.** 2006. SUN-domain proteins: "Velcro" that links the nucleoskeleton to the cytoskeleton. Nat. Rev. Mol. Cell Biol. **7:**782–788.
63. **Ueda, M., R. Graf, H. K. MacWilliams, M. Schliwa, and U. Euteneuer.** 1997. Centrosome positioning and directionality of cell movements. Proc. Natl. Acad. Sci. USA **94:**9674–9678.
64. **Ueda, M., M. Schliwa, and U. Euteneuer.** 1999. Unusual centrosome cycle in *Dictyostelium*: correlation of dynamic behavior and structural changes. Mol. Biol. Cell **10:**151–160.
65. **Valentine, M. T., P. M. Fordyce, and S. M. Block.** 2006. Eg5 steps it up! Cell Div. **1:**31.
66. **Xiang, X., W. Zuo, V. P. Efimov, and N. R. Morris.** 1999. Isolation of a new set of *Aspergillus nidulans* mutants defective in nuclear migration. Curr. Genet. **35:**626–630.
67. **Xiong, H., F. Rivero, U. Euteneuer, S. Mondal, S. Mana-Capelli, D. Larochelle, A. Vogel, B. Gassen, and A. A. Noegel.** 2008. *Dictyostelium* Sun-1 connects the centrosome to chromatin and ensures genome stability. Traffic **9:**708–724.